Extreme wave events in the Gulf of Tehuantepec

W. K. Melville, L. Romero, and J. M. Kleiss

Scripps Institution of Oceanography, University of California San Diego, La Jolla, CA 92093-0213, USA

Abstract. Observations of extreme, "freak" or "rogue waves" have typically depended on chance observations from ships at sea or from fixed oil or gas platforms. The observations have been so sparse that there are very few direct temporal or spatial measurements, and those that do exist are so infrequent that they have often been individually named: e.g. the "Draupner Wave." Such named observations tend to occur every few years. This paucity of data, and the fact that much of it is from fixed platforms, whose location is not optimized for wave research, makes it very difficult to undertake an organized study of the statistics and occurrence of rogue waves over large regions. In this paper we present an alternative approach that uses airborne spatio-temporal wave measurements, along with video imaging, to measure the evolution of waves under strong winds in fetch-limited conditions. Using the criterion that a freak wave has a height $H \geq 2H_s$, where H_s is the significant wave height, during a flight of approximately 8 hours over a 400 km fetch in winds approaching 25 m s^{-1} in the Gulf of Tehuantepec off the Pacific coast of Mexico, we find four freak waves. We describe their spatial structure and the occurrence of breaking.

Introduction

The safe design for the operation of ships at sea and other offshore activities depends on the availability of accurate weather and wave predictions. Of particular interest is the probability of extreme events that can endanger the vessel or platform and their crews. Since practical designs always involve compromises between safety and efficiency, the aim is to account for the expected events over the useful lifetime of the ship or structure, while minimizing the cost of overdesign. For some vessels and platforms, even large but not extreme events may limit operations so that measuring or predicting their occurrence can become an important planning and safety tool.

Freak or rogue waves are in this category of extreme events, and better understanding their characteristics, occurrence and statistics on a regional and seasonal basis is an important goal in surface-wave research. The processes that can lead to large, steep extreme waves include refraction by topography and currents, nonlinear focussing, dispersive focussing and wave-current interaction.

The essential physics of these processes is understood but their occurrence in the ocean is poorly documented. It is well-known that many of the shipping incidents associated with rogue waves occur in regions where large waves and swell meet opposing currents, which tend to steepen and shorten the waves. For example, waves and swell from the Southern Ocean meeting the Agulhas Current have been the cause of shipping losses off the coast of South Africa. However, the exclusion of vessels from this region may be unnecessarily conservative in planning shipping routes.

Satellite remote sensing, especially synthetic aperture radar (SAR) in combination with radar altimetry (e.g., Topex/Poseidon, Jason), is an attractive tool for measuring waves over large regions of the world's oceans. SAR is particularly useful for imaging patterns of the longer waves and wave groups, but there are still issues related to the calibration of the radar backscatter. While significant progress has been made in calibrating SAR imagery, much remains to be done to demonstrate accurate SAR inversion for wave height.

In this paper we wish to describe wave measurements made in the Gulf of Tehuantepec off the Pacific coast of Mexico. The experiments were conducted (in collaboration with Carl Friehe at UC Irvine) to better understand the coupling between the evolution of the marine atmospheric boundary layer and the wave field, especially the incidence of wave breaking. The Gulf of Tehuantepec is well known for the incidence of high winds and waves in the winter months when mountain gap winds blow out from the Gulf of Mexico through a pass in the mountains. In the course of analysis, it became apparent that the wave data may be particularly useful for investigating the incidence of extreme waves under high-wind fetch-limited conditions. Here we present a preliminary analysis of the data in the context of

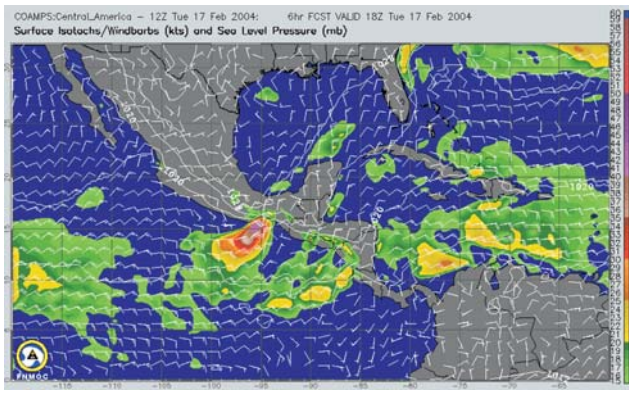

Figure 1. The 30-hr surface wind forecast provided by the Fleet Numerical Meteorology and Oceanography Center (FNMOC) shows contours of wind speed and direction of the jet fanning out from the Gulf of Tehuantepec over the Pacific Ocean on 17 February 2004.

finding and characterizing extreme wave events.

The experiment and instrumentation

The Gulf of Tehuantepec is located off southern Mexico's Pacific coast (Figure 1). When high pressure is over the Gulf of Mexico in the Caribbean, a circulation sets up forcing strong winds through the Chivela mountain pass, creating an off-shore jet over the Pacific Ocean. The wind can blow out for 500-600 km offshore for several days giving rise to strongly-forced fetch-limited wave conditions.

In February 2004, groups from Scripps Institution of Oceanography (UCSD), UC Irvine, NASA/EG&G, NCAR and the National Autonomous University of Mexico collaborated to conduct the Gulf of Tehuantepec Experiment (GOTEX) to measure the coupled development of the atmospheric boundary layer and the surface wave field out over the gulf. The wind jets occur on average about once a week during the winter months, and during the course of GOTEX we measured sustained winds at the coast of 25 m s^{-1}, gusting to 30 m s^{-1}, and decreasing to 10-15 m s^{-1} over a fetch of approximately 500 km. The NSF/NCAR C-130Q Hercules aircraft was equipped with a suite of sensors for measuring surface waves and wave breaking, including a downward-looking scanning lidar (Airborne Terrain Mapper, or ATM), video cameras, inertial motion sensors, and radome gust probe wind measurements. The aircraft, based in Huatulco, was flown in the wind jet starting from the beach at Salina Cruz at the head of the gulf out to fetches of approximately 500 km, at altitudes from 30 to 1500 meters. A typical flight was flown at approximately 100 m s^{-1} with the round trip (out and back) lasting for approximately 8 hours.

The primary instrument for the wave measurements was

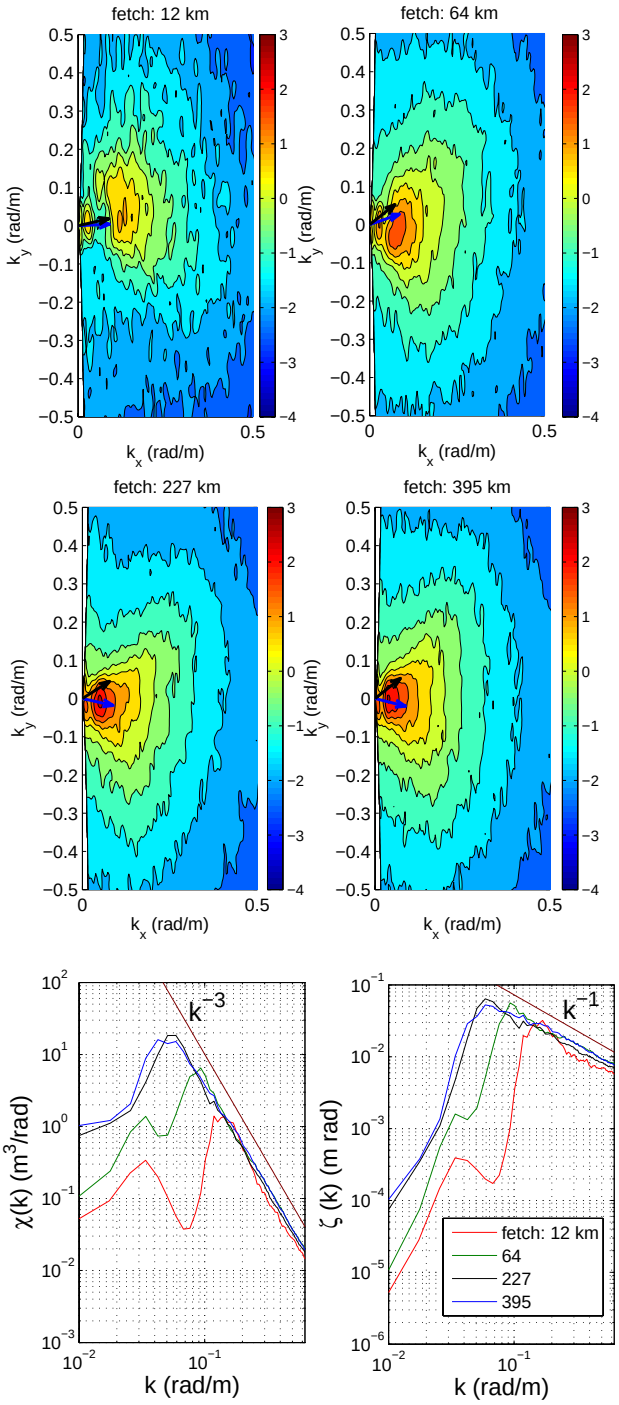

Figure 2. Top panels: contour plots of directional wavenumber spectra ($F(k_x, k_y)$) shown sequentially with increasing fetch. k_x and k_y correspond to the along-track and cross-track wavenumber components, respectively. Blue arrows point in the direction of the wind at a height of 30 m. Black arrows point to true south. Bottom panels: azimuth-integrated (omnidirectional) sea surface height (left) and slope (right) spectra. Solid brown lines are reference spectral slopes proportional to k^{-3} (left) and k^{-1} (right). These results correspond to measurements collected on February 17, 2004.

the NASA Airborne Terrain Mapper (ATM) which is a conical-scanning downward-looking lidar with an off-nadir angle of 15^o. It rotates at 20 Hz and has a pulse repetition rate of 5 kHz. The typical aircraft altitude during ATM operation was 400 m above the mean sea surface. For this altitude the laser has a 0.4 m footprint on the surface, the cross-track horizontal resolution is about 2.5 m and the swath width is about 200 m. The along-track resolution for the typical aircraft velocity of 100 m s^{-1} is about 5 m. For more details see *Hwang* et al. (2000). The ATM vertical rms error is 8 cm, which includes 3 cm (rms) in range, 5 cm rms for positioning through differential GPS, and 5 cm rms for altitude–induced errors (*Krabill and Martin*, 1987). The scanning lidar data was transformed to earth-centered coordinates using aircraft position and altitude data from GPS (global positioning system) receivers and inertial navigation system (INS) sensors.

A nadir-looking Pulnix 1040 megapixel digital video camera was mounted on the aircraft to measure whitecapping produced by breaking waves. Video sequences of sea surface brightness were captured at 15-30 frames per second at a typical aircraft altitude of 300-500 m, giving a footprint of 0.25 m for each pixel edge and 230 m for the image edge (pixels and images were approximately square). Video images were correlated with aircraft motion data by matching the observed image translation to the expected image translation due to aircraft rotation and translation using the method of homography in computer vision (*Ma* et al., 2003). The same aircraft motion data used for the scanning lidar was used to project the video images to earth-centered coordinates, after adjusting for the location of the video camera on the aircraft.

Spectral evolution of the wave field

Before the ATM data is analyzed, it is gridded and interpolated onto a 2.5m by 2.5m grid. Figure 2 shows contour plots of the directional wavenumber spectra $F(k_x, k_y)$, where k_x and k_y correspond to the along-track and cross-track wavenumber components, respectively, obtained from the ATM data on February 17, 2004. The contour plots of $F(k_x, k_y)$ are shown sequentially with increasing fetch of 12, 64, 227 and 395 km, respectively. (True south and the local direction of the 30 m wind are shown by black and blue arrows, respectively.) The omnidirectional sea surface height and slope spectra, $\chi(k) = \int_{-\pi}^{\pi} F(k,\theta)kd\theta$ and $\zeta(k) = \int_{-\pi}^{\pi} F(k,\theta)k^3 d\theta$, respectively, are shown on the bottom panel of Figure 2. At large wavenumbers $\chi(k)$ and $\zeta(k)$ show spectral slopes of k^{-3} and k^{-1}, respectively. The fetch relations for wave height and peak frequency are consistent with the reanalysis of *Kahma and Calkoen* (1992) for stable atmospheric stratification.

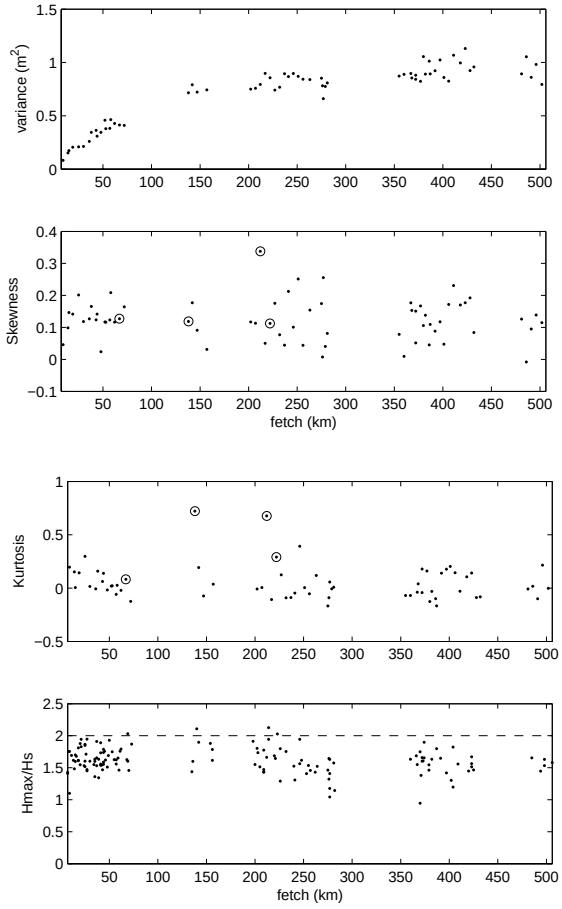

Figure 3. Sea surface statistics and maximum wave heights with fetch. The top three panels show the variance, $V = \langle \eta^2 \rangle$, the skewness, $S = \langle \eta^3 \rangle / \langle \eta^2 \rangle^{3/2}$, and the excess kurtosis, $K = \langle \eta^4 \rangle / \langle \eta^2 \rangle^2 - 3$, for approximately 5-km-long swaths of wave data, where $\langle \eta \rangle = 0$. The bottom panel shows the maximum individual wave heights, H_{max}, normalized by the significant wave height, H_s, for cases when $\eta \geq H_s$. Also shown is the freak-wave threshold of $H_{max} \geq 2H_s$. All data collected February 17, 2004.

Wave statistics and extreme events

Figure 3 shows the variance, $V = \langle\eta^2\rangle$, the skewness, $S = \langle\eta^3\rangle/\langle\eta^2\rangle^{3/2}$, and the excess kurtosis, $K = \langle\eta^4\rangle/\langle\eta^2\rangle^2 - 3$, for approximately 5-km-long swaths of wave data on February 17, 2004, where η is the sea surface displacement and $\langle\eta\rangle = 0$. Also shown is the distribution of H_{max}/H_s as a function of fetch, where H_{max} is the maximum height between the crest and either the back or the front trough aligned in the flight direction. $H_s = 4\langle\eta^2\rangle^{1/2}$ is the significant wave height of the record. Events are analysed for which the largest wave within a group has a crest amplitude greater than H_s. Recall that both the skewness and excess kurtosis are zero for normal distribution. The skewness measures the asymmetry of the distribution, whereas the excess kurtosis measures the peakedness of the distribution function. The data show 4 freak wave events, with many more just below the freak-wave threshold of $H_{max} \geq 2H_s$. However, the threshold in H_{max}/H_s does not appear to correspond to equivalent thresholds in either skewness or excess kurtosis.

Figure 4 shows examples of spatial series approximately 5 km long at fetches of 25, 69, 140, 214, and 423 km, with large wave events for which $1.67 < H_{max}/H_s < 2.13$, of which three are freak waves with $H_{max}/H_s \geq 2$. In all cases the predominant direction of wave propagation is from left to right. The bottom panel of the figure shows the two-dimensional swath and the cut through the swath corresponding to the spatial series at 423 km fetch. The swath clearly shows the large wave has a crest length of 100 m or more, while the wave field is significantly two dimensional in the horizontal plane. The data also show that even at small fetches (25 km) large waves can "pop up out of nowhere", and may prove a danger to smaller vessels. Extreme wave events were detected in this data set not only at relatively short fetch, when the conditions are expected to be favorable for the occurrence as suggested by *Janssen* (2003), but at various fetches. All cases may not strictly meet the criterion for freak waves, but like those examples shown in Figure 4, all are significant events.

One of the important questions concerning freak waves is whether they are breaking. The combination of the ATM and the visible imagery permits this question to be addressed in several of the cases shown in Figure 4. For various reasons, data acquisition for the ATM and the video data stream were not synchronised, and the scan rate of the ATM (20 Hz) and the frame rate of the video camera (15, 30 Hz) are not commensurate. This, along with the speed of the aircraft means that the wave height data from the ATM and the imagery may have position differences of up to 12 m, when attempting to synchronise both sets of data. Nevertheless, Figures 5 and 6 show essentially simultaneous imagery and ATM data for the last two events shown in Figure 4. Contours of foam patches shown in the video image have been superimposed on the ATM data showing breaking along the crest of the large wave at 214 km fetch, and breaking on the forward face of the wave event at a fetch of 423 km. The different phases of the breaking relative to the wave crest may be due in part to the image registration issues mentioned above, or could be physical effects associated with long-wave short-wave interaction or the stage of breaking. Visual observations from the cockpit of the aircraft found that breaking of the shorter waves was often associated with wave-wave interaction. Patches of residual foam are visible in the troughs of the event at 214 km fetch, probably persisting from active breaking along the crest. The close-up wave height profiles in Figures 5 and 6 may not exactly match the 5-km profiles in Figure 4, panels 4 and 5 because of minor differences in the absolute angle of the flight track direction and the determination of $\langle\eta\rangle = 0$ when considering only these shorter flight segments.

Wave-current interaction

As mentioned in the Introduction, it is well known that waves propagating into an opposing current gradient can steepen, shorten and break, and some of the most destructive occurrences of freak waves on shipping have been under such circumstances. While the basic physics of this process is well-understood, and can be formulated in terms of wave-action conservation and geometrical optics, the consequences for wave evolution, especially in the coastal oceans, have perhaps not been fully recognized.

In the top panel of Figure 7 we show a photograph taken on February 19, 2004, from the cockpit of the C-130 showing regions of the ocean surface with breaking and almost no breaking, separated by a narrow region of strong breaking: a "front". This was a serendipitous observation. The pilot was requested to turn around and follow the front for some distance. This was done and the aircraft track is shown in the other panels of the figure overlaying remote sensing of the sea surface temperature on the same day. The correspondence between the thermal front and the observed line of breakers is very good and consistent with the interpretation that the strong line of breakers is due to interaction between the waves and the currents induced by the thermal front. It is well-known that SAR and real aperture radar (RAR) are useful for imaging frontal boundaries due to the interaction between the short ($O(1-10)$ cm) surface waves (the microwave scatterers) and the frontal currents. However, observations of coastal fronts leading to breaking of significantly longer waves, as shown here, have been much less frequent. These data also point to the fact that wind-wave models, for which breaking is an important contributor to the "source" terms, may need to take more complete account of current variability due to fronts, especially in the coastal oceans. To the extent that improved predictions of extreme or freak waves depend on better wave models, higher reso-

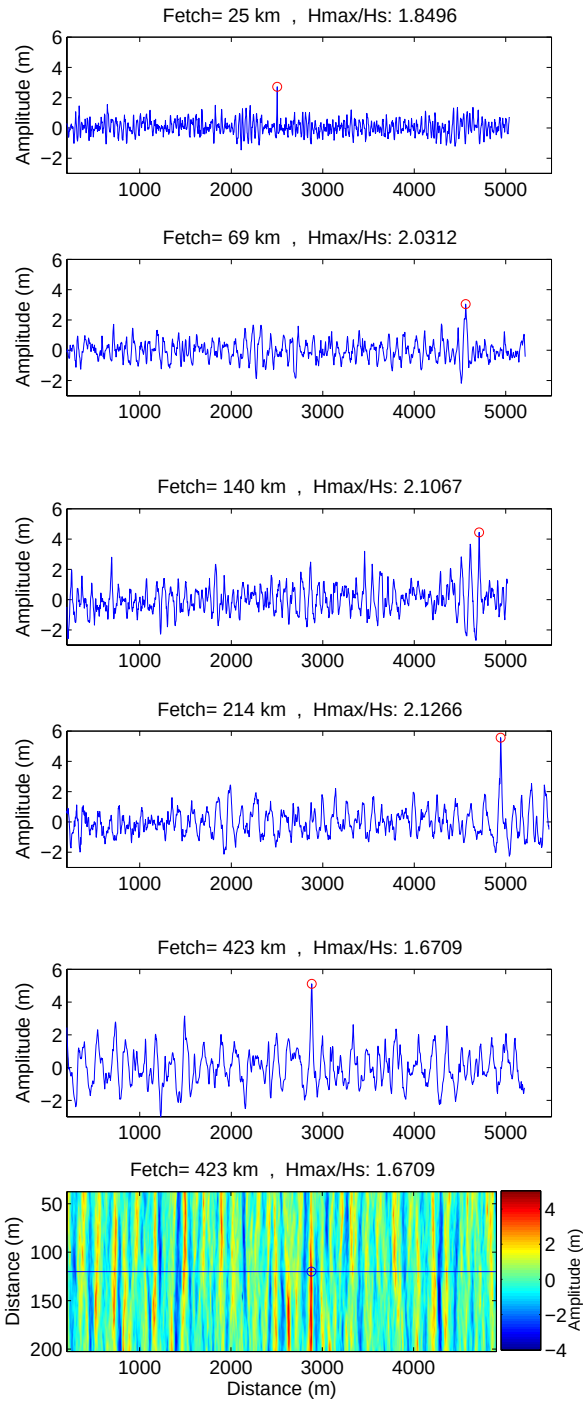

Figure 4. Top five panels: single profiles in the along-flight direction, obtained from 2-dimensional ATM swaths on 17 Feb. 2004, show samples of large waves at various fetch. Large waves were identified whenever $\eta > H_s$, where $H_s = 4\sqrt{\langle \eta^2 \rangle}$ is the significant wave height of the record. Record length is approximately 5 km. Bottom panel: 2-dimensional ATM swath showing the large wave and horizontal cut where the profile on panel five was obtained.

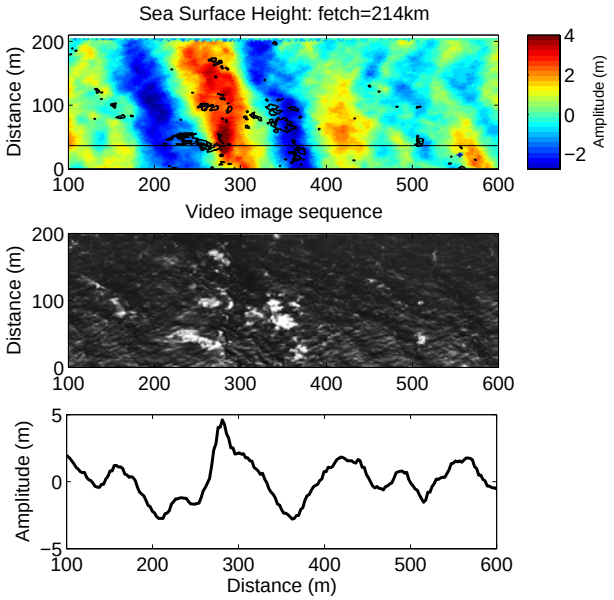

Figure 5. Detail of the large wave example of Figure 4, panel 4 (fetch=214 km). Top panel: detail of sea surface height in the along-flight direction. Middle panel: the corresponding sea surface brightness obtained from video images. Contours of the foam patches are superimposed on the top panel in black. Bottom panel: sea surface displacement profile through the horizonal line indicated in the top panel. Wind, wave, and aircraft velocity are all in the positive x-direction.

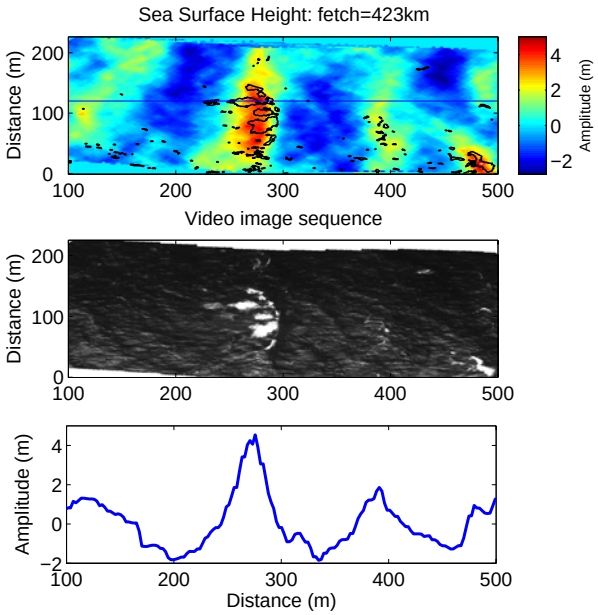

Figure 6. Detail of the large wave example of Figure 4, panel 5 (fetch=423 km). See Figure 5 caption for description.

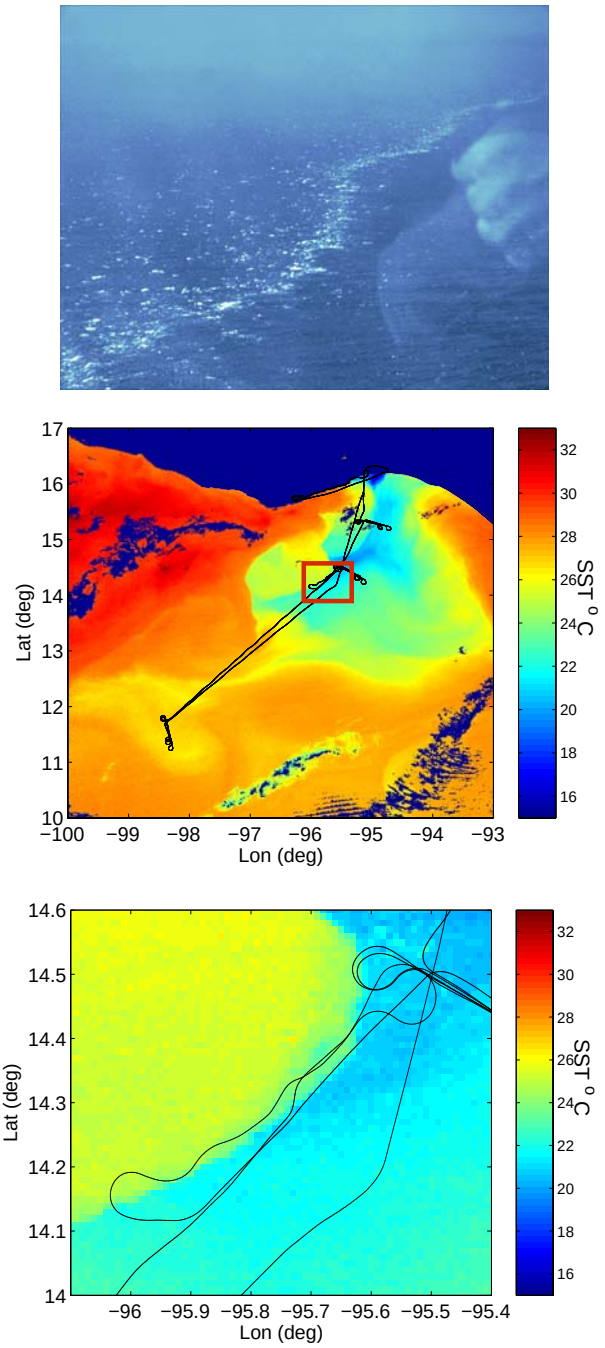

Figure 7. Top panel: photo taken from the aircraft cockpit on February 19, 2004 showing a line of enhanced breaking, as well as the reflection of the photographer's hand. Middle panel: MODIS AQUA Satellite image of sea surface temperature, flight path (black line), and coast (blue region). The red box indicates the flight segment along the line of breaking, which follows a temperature front. Bottom panel: zoom of the area enclosed within the red box. MODIS-Aqua image obtained from: http://daac.gsfc.nasa.gov/data/dataset/MODIS-Aqua/index.html

lution current fields may be required.

Discussion

In this paper we have attempted to demonstrate that improved methods of airborne wave measurement and imaging may significantly increase the data base for studying wave statistics and the occurrence of extreme and freak waves. These methods complement the broad coverage afforded by microwave remote sensing (SAR) while providing a calibrated measurement in space and time. The portability of the airborne methods permits measurements to be made in regions that are known to be prone to freak wave occurrences, and would thereby facilitate significantly improved intercomparisons between observations and process-oriented wave models.

Acknowledgments

We thank Carl Friehe and Djamal Khelif for collaborations in GOTEX. The GOTEX experiment would not have been possible without the dedication and skills of the scientific staff and crew from NCAR/ATD/RAF, and those of Bill Krabill, Bob Swift and their ATM team at NASA/EG&G. This research was supported by NSF(Ocean Sciences) and ONR (Physical Oceanography).

References

Hwang, P., D. Wang, E. Walsh, W. Krabill, and R. Swift, Airborne measurements of the wavenumber spectra of ocean surface waves, Part I: Spectral slope and dimensionless spectral coefficient, *J. Phys. Oceanogr., 30,* 2753–2767, 2000.

Janssen, P. A. E. M., Nonlinear four-wave interactions and freak waves, *J. Phys. Oceanogr., 30,* 863–884, 2003.

Kahma, K. K., and C. J. Calkoen, Reconciling discrepancies in the observed growth of wind-generated waves, *J. Phys. Oceanogr., 30,* 1389–1405, 1992.

Krabill, W., and C. Martin, Aircraft positioning using global positioning carrier phase data, *Navig., 34,* 1–21, 1987.

Ma, Y., S. Soatto, J. Kosecka, and S. Sastry, *An Invitation to 3–D Vision: From Images to Geometric Models,* Springer-Verlag, New York, 2003.

This preprint was prepared with AGU's LaTeX macros v4, with the extension package 'AGU^{++}' by P. W. Daly, version 1.6a from 1999/05/21.